

Edge Computing Based Multi-Objective Task Scheduling Strategy for UAV with Limited Airborne Resources

Xiaoqiang Wang

Chinese-German College of Engineering, Shanghai Technical Institute of Electronics & Information, Shanghai, 201411, China

Email of corresponding author: wxqfyc@163.com

Keywords: unmanned aerial vehicle, edge computing, limited airborne capacity, multi-objective, task scheduling

Received: March 11, 2024

The unmanned aerial vehicles often suffer from insufficient computing power due to the limited onboard resources, resulting in task delays under heavy tasks. A system based on edge computing was constructed to solve this problem, which involved task allocation center, unmanned aerial vehicle group, data node, and power supply station. A mathematical optimization framework based on task, resource, and scheduling models was proposed, and the non-dominated sorting genetic algorithm III was used. The objective optimization was efficiently processed through genetic operations, non-dominated sorting, and reference point-based selection mechanisms. These results confirmed that the non-dominated sorting genetic algorithm III performed well in comprehensive performance evaluation, with an MS index of 0.881 in large-scale map tests and an AQ index of 0.133 in medium-sized maps. The calculation time was 58.9 seconds, 140.5 seconds, and 545.3 seconds in small, medium, and large map tests, respectively, leading other algorithms. Therefore, the designed model has excellent performance in task quality, time extension, and computational efficiency, which has application value.

Povzetek: Študija uporablja sistem temelječ na robnem računalništvu, za načrtovanje večnivojskih nalog za brezpilotna letala z omejenimi viri je uveden sistem, temelječ na robnem računalništvu, ki dosega visoko točnost in učinkovitost pri razporejanju nalog.

1 Introduction

In the era of highly developed technology, Unmanned Aerial Vehicle (UAV) has become an important research field, with applications ranging from military, investigation, daily delivery to ecological research, and more. The onboard resource management of the UAV operation becomes an important technical challenge. This includes many aspects of UAV power management, load scheduling, flight path design, etc. [1-3]. Especially, how to effectively carry out task scheduling to ensure optimal operational efficiency and task completion quality becomes an important research topic under limited airborne resource conditions. In task scheduling, UAV needs to ensure optimal allocation of system resources while executing tasks to achieve maximum work efficiency [4-6]. With the development of big data and cloud computing, edge computing becomes a hot research field in recent years. Edge computing can solve the high data transmission delay, data loss, and security in cloud computing. Edge computing is an important technical strategy to support efficient operation of UAV in complex environments. Previous studies have mostly focused on single task scheduling strategies, with less attention paid to multi-task scheduling problems under limited resource conditions [7-9]. Therefore, this study

aims to analyze the edge computing-based multi-target task scheduling strategy under the condition of limited UAV airborne resources. It is hoped to provide new theoretical support and practical reference for the task scheduling strategy of UAV. The research mainly includes four parts. Firstly, the research objective is proposed. Then, a multi-objective task scheduling strategy for UAV is designed. Next, model validation is conducted. Finally, a conclusion is drawn.

2 Research background

As UAV continues to evolve, the task scheduling research gradually deepens. You W et al. designed an optimization model aimed at minimizing the total energy consumption of user UAV. Meanwhile, an iterative algorithm using block coordinate descent method was proposed, which had high efficiency [10]. Halder et al. proposed a novel clustering method that enabled UAV to achieve dynamic task scheduling. The throughput optimality of its scheduling algorithm was determined through the Lyapunov drift analysis framework. These experiments confirmed that the proposed method surpassed existing solutions in terms of energy consumption, cluster overhead, throughput, end-to-end latency, flow success rate, and packet loss rate [11]. Niu Z et al. discussed how to better utilize UAV for task

scheduling in disaster scenarios. They suggested using a decentralized computing network consisting of UAV and ground mobile devices. These results confirmed that their algorithm reduced the energy consumption of the entire system by more than 50% while ensuring queue stability [12]. Wang Y et al. proposed a mixed integer nonlinear programming model. Meanwhile, an alternating optimization algorithm was proposed based on differential evolution and greedy Hongya algorithm to obtain suboptimal solutions. These experiments confirmed that the total benefit of this scheme was approximately 50% higher than existing methods [13].

On the other hand, the application of Non-dominated Sorting Genetic Algorithm III (NSGA-III) gradually diversifies and deepens. Khettabi I et al. used the new dynamic Non-dominated Sorting Genetic Algorithm II (NSGA-II) and the new NSGA-III for evaluation. The effectiveness of the proposed method was demonstrated through three measurement criteria. Finally, TOPSIS was used to assist decision-makers in evaluating and selecting the best process plan [14]. Awad M et al. aimed to use NSGA-II and its extended version to solve single

objective and Multi-objective Optimization (MOO) problems and find Pareto optimal solutions in stock investment portfolio management. These experiments confirmed that NSGA-II was effective for portfolio problems with two objective functions, while NSGA-III was effective for problems with three objective functions [15]. Johnson N N et al. investigated the influence of welding parameters on solder joint quality and combined Kriging and the new NSGA-III for MOO of RSW. These experiments confirmed that optimized welding parameters effectively improved the welding quality. When using the optimized welding parameters, the concave diameter, tensile shear strength, and peel strength of the welded specimens increased by about 9.21%, 4.95%, and 7.69%, respectively [16]. Harif S et al. proposed four conflicting optimization objectives using NSGA-III to improve the ideal position of sensors. These experiments confirmed that as the sensors increased, the Pareto front became more effective [17]. The literature summary is shown in Table 1.

Table 1: Literature summary

Author	Research dimensions	Research contents	Research conclusion	Literature
You et al.		Designed an optimization model aimed at minimizing the total energy consumption of user UAV	This method has higher efficiency compared to existing solutions	[10]
Halder et al.	UAV task scheduling	Proposed a clustering method for UAV dynamic task scheduling	This method performs excellently in terms of energy consumption, cluster overhead, throughput, end-to-end latency, and packet loss rate	[11]
Niu et al.		Analyzed UAV task scheduling methods in disaster scenarios	The model reduces the energy consumption of the entire computing system by more than 50% while ensuring queue stability	[12]
Wang et al.		A mixed integer nonlinear programming model was proposed.	The overall return of this plan is 50% higher than that of existing methods	[13]
Khettabi et al.	Application of NSGA-III model	Proposed evaluation methods for new dynamic NSGA-II and new NSGA-III	The effectiveness of the method is demonstrated through three measurement standards	[14]

Awad et al.	Expanded and applied the NSGA-II model to solve single objective and multi-objective optimization problems.	Solved the combination problem of two objective functions and three objective functions	[15]
Johnson et al.	Multi-objective optimization of RSW using Kriging and the new NSGA-III model	After using optimized welding parameters, the concave diameter, tensile shear strength, and peel strength of the welded samples all increased.	[16]
Harif et al.	Proposed four optimization objective functions based on NSGA-III to improve the placement of sensors	Obtained better monitoring results	[17]

In conclusion, many researchers focus on the task scheduling strategy on UAV, mobile edge computing and solving optimization problems. Some researchers have designed optimization problems to reduce the total energy consumption of UAV by constructing layered systems. Some have explored how to use UAV for task scheduling in disaster scenarios. Some scholars have also emphasized the role of UAV in dynamic task scheduling, optimal UAV deployment, and mobile device location determination. Meanwhile, the application of NSGA-III has also been promoted in many fields, such as reconfigurable manufacturing systems, portfolio management, manufacturing, and so on. This study further considers the UAV task allocation that UAV may face under limited loads on the basis of the existing research mentioned above, providing a new approach for this field. This study not only solves the limited airborne problem, but also solves the task scheduling problem under limited computing power. A comprehensive model performance evaluation is conducted, providing a more efficient solution for real-time task scheduling under limited resources.

3 Design of unmanned aerial vehicle multi-objective task scheduling strategy

A MOO-UAV scheduling mathematical model is proposed to address the computational power shortage and task delay caused under limited airborne conditions. This model consists of tasks, resources, and scheduling models and is optimized and solved using NSGA-III.

3.1 Architecture of task scheduling model

The MOO-UAV system is built on the edge computing framework. This system mainly includes the following main components: task allocation center, UAV group, data node, and power supply station. The MOO-UAV system also includes some abstract elements, including the study of expected optimization goals, various constrainable conditions, and strategy algorithms for solving problems. Figure 1 shows this system.

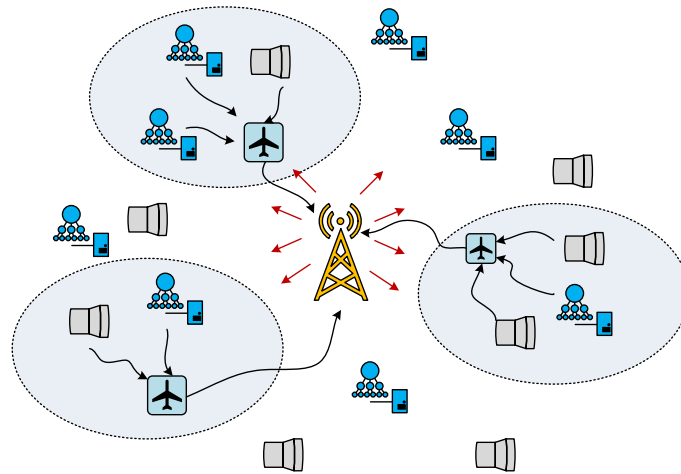


Figure 1: System model

The control center is responsible for supervising all UAV and assigning tasks to them in real-world physical elements. When a data node generates a request, the control center will analyze information such as node location and data size based on this. Then tasks are assigned to each UAV. The control center also serves as a power supply station, as well as takeoff and landing points. UAV is the carrier and processor of data tasks. Each UAV is equipped with a complete set of equipment such as flight control system, wireless communication system, navigation system, etc. The equipment is used for data processing and information transmission during

navigation. The data node is responsible for providing data tasks and transmitting tasks to the UAV during hovering. The power supply station is responsible for supplying UAV energy. In non-physical elements, the optimization objective is to optimize multiple objectives. As a result, the total range of all UAV, the total completion time of data tasks, and the total duration of all overtime tasks can be minimized. Attention should be paid to constraints such as UAV flight speed, power consumption, and range during the solving process. It is crucial to choose the appropriate optimization algorithm for this issue. Figure 2 shows the complete workflow.

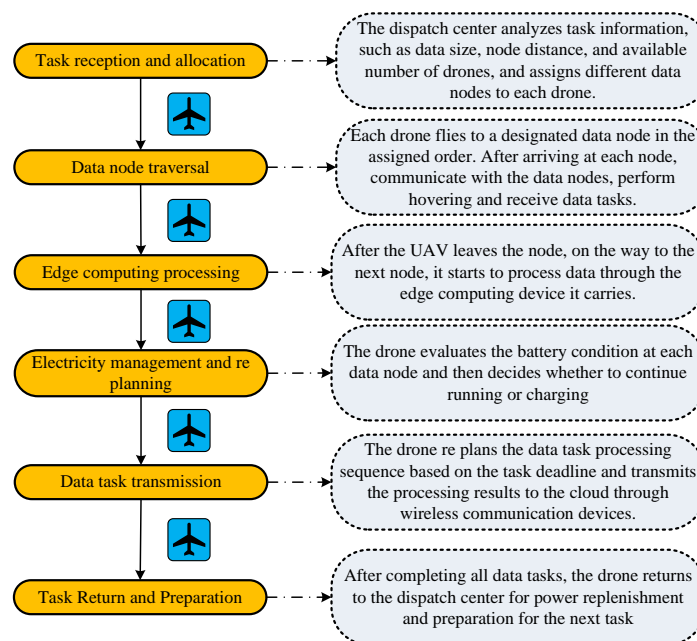


Figure 2: Workflow

The dispatch center will allocate tasks based on various factors such as task information and the number

of UAV after receiving a batch of pending data tasks. The UAV traverses' nodes in the order assigned, hovers over

each node and receives tasks, and then processes data tasks while flying to the next node. If the battery is low, UAV needs to go to the power supply station to replace the battery before continuing the task. UAV returns to the dispatch center to prepare for the next task after completing the task. It is necessary to optimize the route of UAV to minimize the task completion time and voyage during this process, while completing as many tasks as possible.

3.2 Construction of task scheduling operation model

The biggest challenge when scheduling UAV is to find a solution that is suitable for assigning UAV to a large amount of data tasks. Therefore, the timely completion of all tasks can be ensured, and the scheduling cost of UAV can be reduced as much as possible. Therefore, a redesigned MOO-UAV scheduling mathematical model is adopted in this study. It mainly consists of tasks, resources, and scheduling models.

Firstly, a task model is designed, and a scheduling hub is established as the initial stopping point for all UAV, with many data nodes. Each data node has its own

unique task data volume. The data scale for each node is generated through normal distribution to simulate the real-world environment. Then, a resource model is established, including all UAV and edge computing devices. All UAV stay at the dispatch hub at the beginning. The flight speed, data transmission speed, processing speed, and total endurance time of UAV are all known. The endurance time is a key parameter as it determines the number of tasks that a UAV can perform at once. Then, a scheduling model is studied and constructed. Charging stations are set up in the data node area considering the endurance capability of UAV in this model. Meanwhile, UAV generates specific flight paths based on task sequences and base station positions. Then constraints are defined to ensure that the remaining endurance time of UAV at the data node cannot be negative. UAV must have sufficient energy to return to the dispatch center or transfer to the charging station. The optimization objective of this study is to minimize the completion time of data tasks, the total flight path of all UAV, and the total duration of all timeout tasks. Figure 3 shows task scheduling assumptions and constraints.

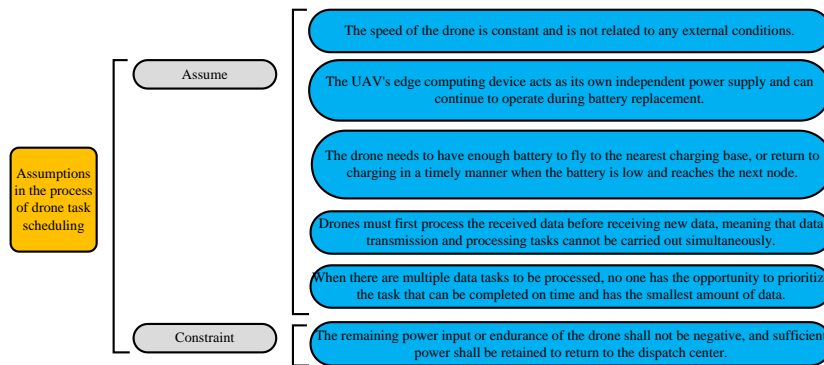


Figure 3: Task scheduling assumptions and constraints

It is assumed that formula (1) is the flight path of UAV.

$$L_j = \{l_{j,1}, l_{j,1}, \dots, l_{j,\tau}\} \quad (1)$$

In formula (1), τ refers to the number of destinations. The constraints of the model are represented by formula (2).

$$t_{j,\tau}^{r,e} \geq \frac{D(l_{j,q}, B_{j,q})}{v} + h_{j,\tau} \quad (2)$$

In formula (2), $l_{j,q}$ refers to the destination of the UAV. v refers to the speed. j refers to the number of UAV. $B_{j,q}$ refers to the nearest charging station. $h_{j,\tau}$ refers to the estimated electricity consumption from the

node to the dispatch center. D refers to the distance. Further, formula (3) can be obtained.

$$t_{j,\tau}^{r,e} = \begin{cases} t^{\max} \\ t_{j,\tau-1}^{r,e} - h_{j,\tau-1} - \frac{D(l_{j,q}, B_{j,q-1})}{v} \end{cases} \quad (3)$$

In formula (3), t^{\max} refers to the maximum endurance time. Formula (4) is used for constraints due to the fact that the ultimate destination of the UAV is a data node, which is not a charging station.

$$N_j \notin B \quad (4)$$

In formula (4), B refers to the charging station. The study adopts MOO methods suitable for three objectives and higher to evaluate the final benefits. Therefore, the flight path of UAV, dwell time at all nodes,

and other data processing time can be minimized after the end of the last data task. The completion time of UAV tasks is represented by formula (5).

$$t_j^{fin} = \sum_{q=2}^{N_j} \left(\frac{D(l_{j,q-1}, B_{j,q})}{v} + h_{j,q} \right) + \sum_{\rho=1} Z_{N_{j,\rho}} \quad (5)$$

In formula (5), N_j refers to the total destinations.

$D(l_{j,q-1}, B_{j,q})$ refers to the distance between different

destinations. $h_{j,q}$ refers to the hover time. $Z_{N_{j,\rho}}$

refers to the pending task for the last data point. The objective function is represented by formula (6).

$$f(x) = \min [f_1(x), f_2(x), f_3(x)]^T \quad (6)$$

In formula (6), $f_1(x)$ refers to the highest

completion time. $f_2(x)$ refers to the total flight

distance. $f_3(x)$ refers to the duration of task timeout.

$f_1(x)$ is represented by formula (7).

$$f_1(x) = \max [t_1^{fin}, t_2^{fin}, \dots, t_n^{fin}] \quad (7)$$

In formula (7), t_n^{fin} refers to the completion time of

the task. $f_2(x)$ is represented by formula (8).

$$f_2(x) = \sum_{j=1}^n \sum_{q=2}^{N_j} D(l_{j,q-1}, l_{j,q}) \quad (8)$$

$f_3(x)$ is represented by formula (9).

$$f_3(x) = \sum_{i=1}^m t_i^{out} \quad (9)$$

In formula (9), t_i^{out} refers to the timeout time.

3.3 Design of multi-objective solving strategies

The MOO algorithm demonstrates strong superiority in handling single objective and multi-objective problems. However, a more powerful MOO tool, namely NSGA-III, is required for increasingly common problems involving three objectives or MOO. NSGA-III is a multi-objective evolutionary algorithm based on reference points, which emphasizes non-dominant population members more than NSGA-II. This method also adds a set of individual related reference points to select the next population individual. As a result, better convergence and diversity can be achieved to find non-dominant solutions. Figure 4 shows the process of the model.

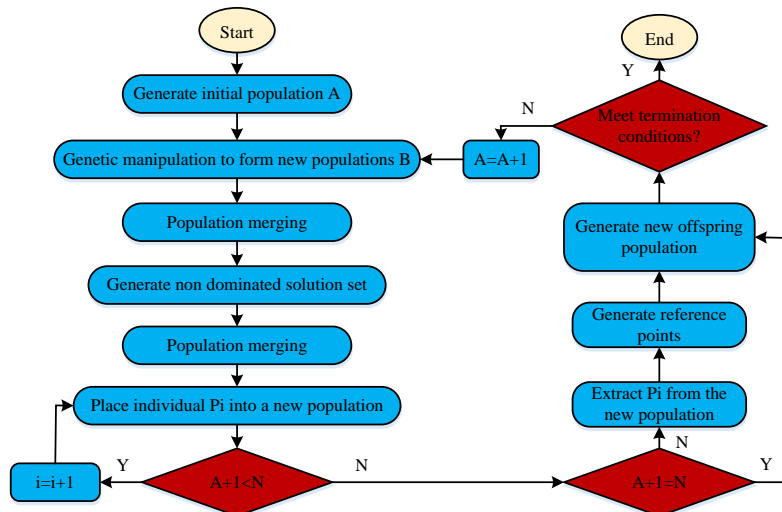


Figure 4: Model process

The execution of NSGA-III requires generating an initial solution using the roulette wheel algorithm, which is the initial population P0 of size H. Then NSGA-III begins genetic operations on the initial solution population, including mutation, crossover, and individual

selection, to generate an iterative population algebra gmax. Genetic operations, non-dominated sorting operations, reference point generation, and the association between individuals and reference points are important components of NSGA-III. Genetic

manipulation involves two types of mutations and one crossover approach. Genetic manipulation aims at maintaining genetic diversity while preserving excellent

gene fragments. Figure 5 shows the mutation and crossover processes.

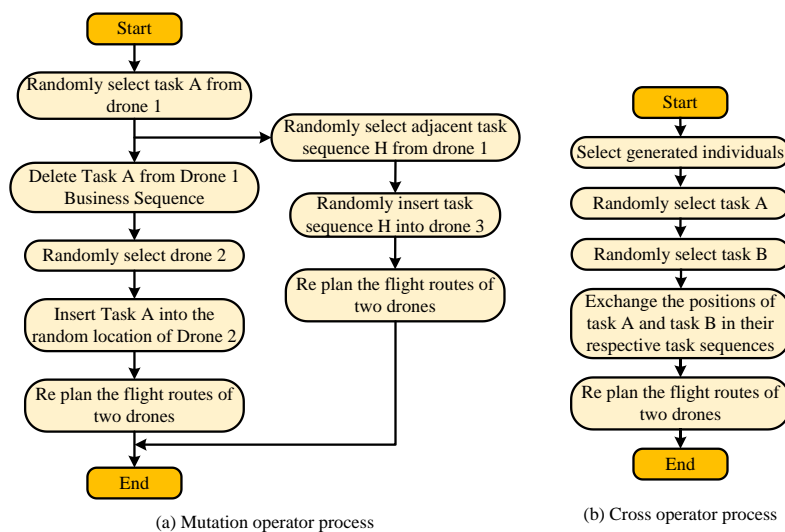


Figure 5: Variations and cross processes

This step preserves certain UAV flight sequences of outstanding individuals and adds them to the sequences of other UAV. Meanwhile, it is crucial to determine the reference point in NSGA-III. The generated new population and parent population form a mixed population after mutation and crossover. All individuals are added to the offspring population after non-dominated sorting is performed on the mixed population to generate multiple non-dominated layers. This step stops until the offspring size exceeds half of the mixed population size. In this process, the study does not use congestion ranking

in NSGA-II, but instead uses a reference point-based method for ranking. The association between individuals and reference points is a crucial step in forming a new population. This solution is to associate all individuals with a reference point, starting from the ideal point and extending infinitely to all reference points. Each line represents a reference line corresponding to a reference point. Figure 6 is a schematic diagram of the reference line.

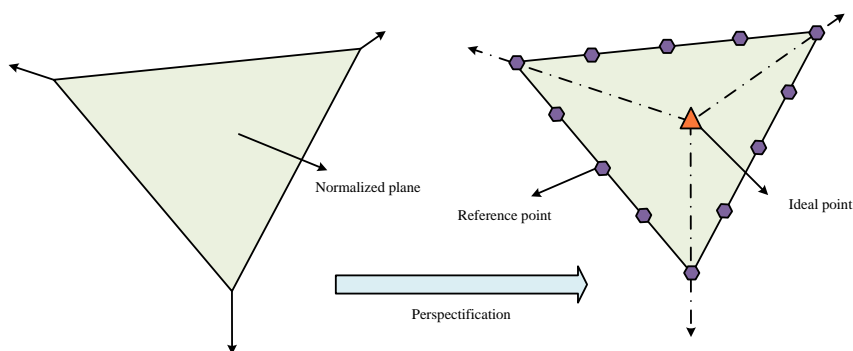


Figure 6: Reference line diagram

Then the closest distance between each individual and all reference lines is calculated. The closest reference point is the individual's associated reference point. Sometimes, a reference point may be associated with one or more individuals, or there may be no individual associated with it. The total reference points in the target

problem are represented by formula (10).

$$H = \binom{M + p - 1}{p} \tag{10}$$

In formula (10), M represents the number of objective problems. If a three-objective problem is adopted, M is 3. P represents population. The

research prioritizes selecting reference points with fewer associated individuals to ensure the diversity of individual populations. Meanwhile, the associated individuals are added to the offspring population. The minimum value of the total duration is represented by formula (11).

$$MIN = \begin{cases} z_1^{\min} \\ z_2^{\min} \\ z_3^{\min} \end{cases} \quad (11)$$

In formula (11), z_1^{\min} represents the maximum and minimum completion time. z_2^{\min} represents the shortest flight length. z_3^{\min} represents the total timeout duration. Therefore, the reference plane zero point in formula (12) can be formed.

$$Z_0 = (z_1^{\min}, z_2^{\min}, z_3^{\min}) \quad (12)$$

When the population is adaptively normalized, the maximum objective value in the three objective problem is normalized and represented by formula (13).

$$f'_i(x) = f_i(x) / z_i^{\max}, (i = 1, 2, 3) \quad (13)$$

In formula (13), z_i^{\max} represents the maximum target value. The individual target dimensions are fixed and the extremum is determined, represented by formula

(14).

$$ASF(x, \omega) = \max_{i=1}^M f'_i(x) / \omega_i, x \in S_x, \omega = (\tau, \dots, \tau, 1, \tau, \dots, \tau), \tau = 10^{-6} \quad (14)$$

After determining the maximum values of all target dimensions, the minimum value is selected as the extremum point, represented by formula (15).

$$Z_i^{\max} = \min \{ ASF(x_1, w_i), ASF(x_2, w_i), ASF(x_3, w_i) \} \quad (15)$$

The individuals are associated with the reference point after normalizing all individuals with the reference point. Priority is given to selecting reference points with fewer associated individuals in the set to add to the offspring population, thereby improving individual diversity of the population.

4 Verification of the effectiveness of traffic flow prediction models

The study first conducted parameter analysis when testing the effectiveness of traffic flow prediction models. Afterwards, an overall model efficiency analysis was conducted. Four multi-objective indicators: Average Quality (Aq), Maximum Spread (Ms), Maximum Distance (Md), and Average Distance (Ad) were used.

4.1 Parameter analysis

In this experiment, the UAV underwent three different configuration settings. Firstly, the study set constants such as UAV endurance time and flight speed. Table 2 shows the experimental setup.

Table 2: Experimental setup

Drone parameters		Option 1	Option 2	Option 3
Drone settings	Battery life (seconds)	800	1000	1200
	Flight speed (meters/second)	20	30	40
	Data transmission speed (minutes)	Θ*0.20	Θ*0.15	Θ*0.10
	Data processing speed (minutes)	Θ*0.50	Θ*0.33	Θ*0.25
Map node settings	Map type		Aponym	Number of nodes
	Small-sized		att48	48
	Medium-sized		bier127	127
Map Type Settings	Large-sized		att532	532
	Map type		Describe	
	Middle		The logistics dispatch center is located in the center of the map	
	Side		The logistics dispatch center is located on the edge of the map	
	Inside		The logistics dispatch center is located at a random location within	

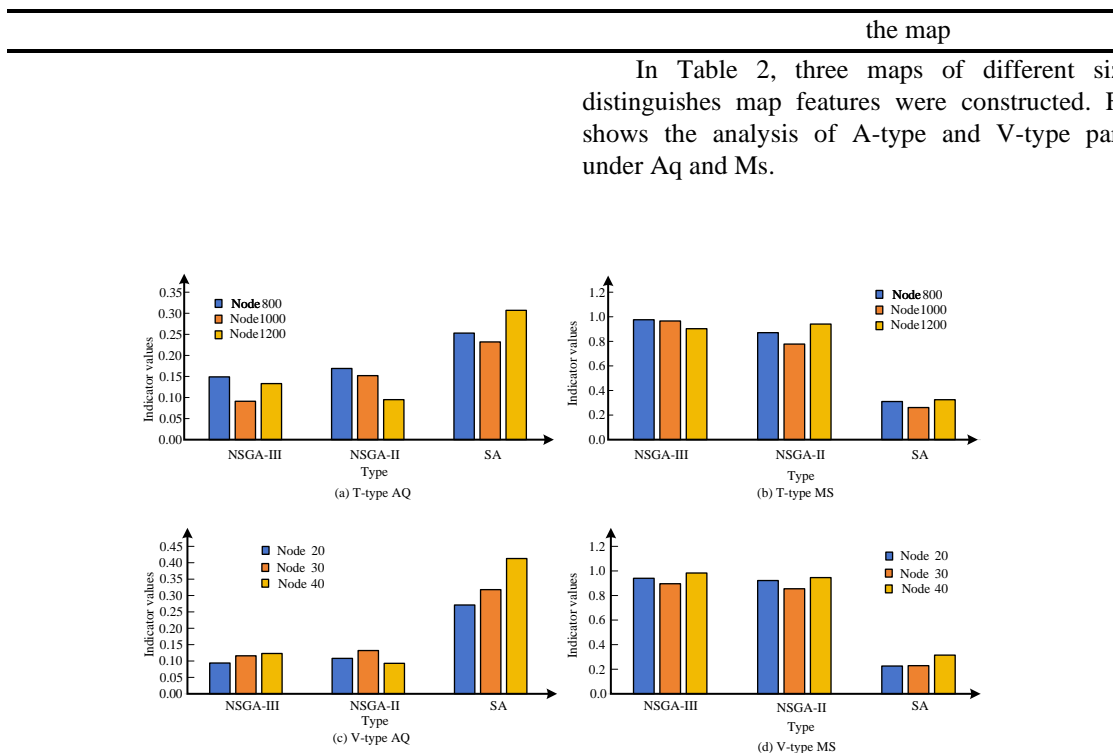


Figure 7: Analysis of A-type and V-type parameters under AQ and MS

In Figure 7, the comparison models are NSGA-II and Improved Simulated Annealing Algorithm (SA), respectively. The study analyzed the effectiveness of UAV task allocation models based on the provided data. The study focused on comparing the performance of different algorithms under specific multi-objective indicators. The indicators considered include Aq and Ms, while the analyzed algorithms are NSGA-III, NSGA-II, and SA. When the nodes were 800, NSGA-III showed a high efficiency of 0.149 on Aq through the analysis of

T-shaped parameters, which was better than NSGA-II's 0.169 and SA's 0.253. Therefore, NSGA-III had better processing ability for UAV task allocation. On MS, NSGA-III was 0.976, leading NSGA-II at 0.871 and SA at 0.31. This trend was also maintained when the parameters increased to 1000, with AQ and MS of NSGA-III being 0.091 and 0.966, respectively, while NSGA-II and SA performed less well. In Table 3, the remaining indicators under Aq and Ms were compared.

Table 3: Comparison of remaining indicators under AQ and MS

Parameter types	Nodes	Aq			Ms		
		NSGA-III	NSGA-II	SA	NSGA-III	NSGA-II	SA
F-type parameter	Middle piece	0.1	0.146	0.307	0.974	0.813	0.263
	Broadside	0.089	0.135	0.299	0.964	0.938	0.314
	Internal	0.124	0.141	0.221	0.906	0.873	0.348
Map parameters	48	0.126	0.103	0.333	0.92	0.921	0.336
	127	0.133	0.096	0.411	0.902	0.937	0.303
	532	0.137	0.17	0.358	0.881	0.87	0.299
T-trans	0.2	0.082	0.166	0.41	0.925	0.93	0.224
	0.15	0.126	0.162	0.336	0.943	0.948	0.3
	0.1	0.105	0.126	0.28	0.848	0.925	0.326
T-pro	0.5	0.145	0.15	0.322	0.875	0.883	0.241
	0.33	0.131	0.116	0.312	0.9	0.888	0.191
	0.25	0.114	0.126	0.293	0.934	0.97	0.266

Merge average	-	0.119	0.133	0.316	0.926	0.901	0.283
---------------	---	-------	-------	-------	-------	-------	-------

In Table 3, NSGA-III performed better with an Aq of 0.1 and a MS of 0.974 for the F-type parameter at the middle node, which were higher than NSGA-II and SA. This indicated that NSGA-III was superior in balancing quality and scalability when dealing with intermediate node tasks. The analysis of side nodes and internal nodes also showed a similar trend, with the Aq of NSGA-III for side nodes being 0.089 and MS being 0.964, both in a leading position. In the evaluation of map parameters, an increase of nodes had a negative impact on the Aq of NSGA-II and SA. However, NSGA-III maintained relatively stable performance, with Aq values gradually increasing from 0.126 to 0.137. This indicated the better robustness of NSGA-II compared to other algorithms. The MS of NSGA-III was 0.881, especially when the

nodes were 532, which was better than NSGA-II and SA. In addition, as the parameter values decreased from 0.2 to 0.1, the Aq performance of NSGA-III remained stable, ranging from 0.082 to 0.105, while MS increased from 0.41 to 0.848. This reflected the algorithmic adaptability to various task scheduling scenarios. When the parameter value decreased from 0.5 to 0.25, NSGA-III also exhibited more robust Aq performance compared to NSGA-II and SA for the T-pro parameter category, with a decrease from 0.145 to 0.114. NSGA-III also maintained an advantage in Ms, rising from 0.875 to 0.934. NSGA-III exhibited overall better performance based on comprehensive analysis of all parameter categories. Its comprehensive average Aq was 0.119, which was significantly lower than NSGA-II's 0.133 and SA's 0.316. The comprehensive average of MS was 0.926, which was the highest among all algorithms. Table 4 shows the comparison of indicators under Davg and Dmax.

Table 4: Comparison of indicators under Davg and Dmax

Parameter types	Nodes	Md			Ad		
		NSGA-III	NSGA-II	SA	NSGA-III	NSGA-II	SA
F-type parameter	Middle piece	0.018	0.015	0.539	0.099	0.066	0.654
	Broadside	0.009	0.016	0.72	0.104	0.083	0.663
	Internal	0.012	0.022	0.553	0.115	0.148	0.732
T-trans	0.21	0.01	0.021	0.688	0.138	0.078	0.857
	0.16	0.009	0.015	0.663	0.098	0.091	0.783
	0.11	0.012	0.018	0.585	0.089	0.123	0.834
T-pro	0.51	0.009	0.022	0.563	0.133	0.148	0.874
	0.34	0.009	0.015	0.611	0.106	0.132	0.866
	0.26	0.008	0.024	0.742	0.085	0.123	0.823
V-shaped	21	0.008	0.022	0.536	0.135	0.064	0.698
	31	0.013	0.015	0.672	0.117	0.089	0.713
	41	0.015	0.026	0.597	0.133	0.083	0.765
T-shaped	805	0.027	0.021	0.361	0.141	0.083	0.791
	1005	0.017	0.016	0.572	0.084	0.096	0.816
	1205	0.009	0.024	0.664	0.124	0.134	0.893
Map parameters	49	0.01	0.017	0.713	0.096	0.073	0.856
	128	0.015	0.021	0.627	0.133	0.138	0.71
	533	0.021	0.022	0.558	0.132	0.12	0.726
Merge average	-	0.013	0.02	0.609	0.115	0.104	0.781

In Table 4, NSGA-III performed better for F-type parameters than the other two algorithms in terms of Ad index. The values of NSGA-III were 0.018, 0.009, and 0.012, respectively, whether in the middle, side, or interior, which were much lower than SA's 0.539, 0.72,

and 0.553. This indicated that the average delay of NSGA-III was lower, and the task allocation efficiency of UAV was higher under F-type parameters. NSGA-III performed for the T-trans parameter better on Ad than the

other two algorithms, whether the node was 0.21, 0.16, or 0.11. The values of NSGA-III were 0.01, 0.009, 0.012, and the SA values were 0.021, 0.015, and 0.018, respectively. However, the performance of these three algorithms was almost the same in terms of Md, with only slightly higher SA, at 0.857, 0.783, and 0.834, respectively. The situation was different for T-pro. Although NSGA-III still outperformed the other two algorithms on Davg, the values of SA on Md were 0.874, 0.866, and 0.823, all higher than those of NSGA-III. This indicated that SA had a higher maximum delay under T-pro, and the efficiency of UAV in executing tasks needed to be improved. NSGA-III still showed a leading advantage in Ad for the V-shaped parameter group, with values of 0.008, 0.013, 0.015, and SA values of 0.536, 0.672, and 0.597. However, on Md, SA exhibited higher latency. Whether the node was 805, 1005, or 1205, NSGA-III had a better value on Ad than SA for the T-type parameter group. However, SA had a higher value

than NSGA-III on Md. Finally, whether the node was 49, 128 or 533, NSGA-III had better values on Ad than SA for the map parameter group. SA had higher values than NSGA-III on Md. The NSGA-III UAV multi-objective task allocation model performs better than the other two models in most scenarios and parameters through the above comparison, with particularly outstanding performance in average latency.

4.2 Efficiency comparison of models

Six different optimization models were compared, including Improved Ant Colony Optimization (IAC), Improved Genetic Algorithm (IGA), Improved Particle Swarm Optimization (IPSO), and Improved Deep Learning Optimization (IDLO). The difference in computation time for completing map data tasks of the same scale is shown in Figure 8.

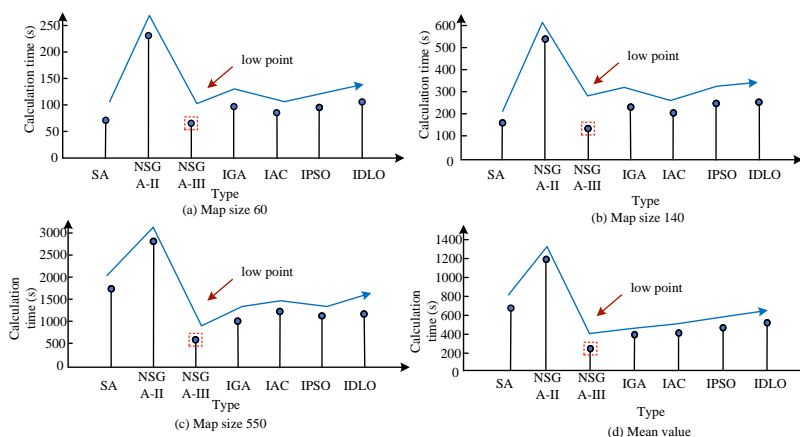


Figure 8: Calculation time difference

In Figure 8, NSGA-III showed a significant efficiency advantage among all algorithms, with the lowest average computation time across all map sizes, only 248.2 seconds. NSGA-III exhibited significant computational efficiency compared to other algorithms. The computation time of NSGA-III was 58.9 seconds on the minimum map size. The closest IAC and SA had a computation time of 70.2 and 85.3 seconds, respectively. The time for NSGA-III was 140.5 seconds on a medium map size, while the time for other algorithms ranged from 158.9 to 252.5 seconds. NSGA-III maintained the shortest computation time of 545.3 seconds on the

maximum map size. NSGA-III significantly reduced computation time by more than 40% compared to SA's 950.5 seconds for the second shortest time. On average, NSGA-III was 192.6, 165.0, 230.3, and 254.8 seconds faster than IGA, SA, IPSO, and IDLO, respectively. This obvious time-saving effect revealed that NSGA-III's algorithm efficiency was higher when facing complex task scheduling with multiple objectives. Figure 9 shows a comparison of task execution times.

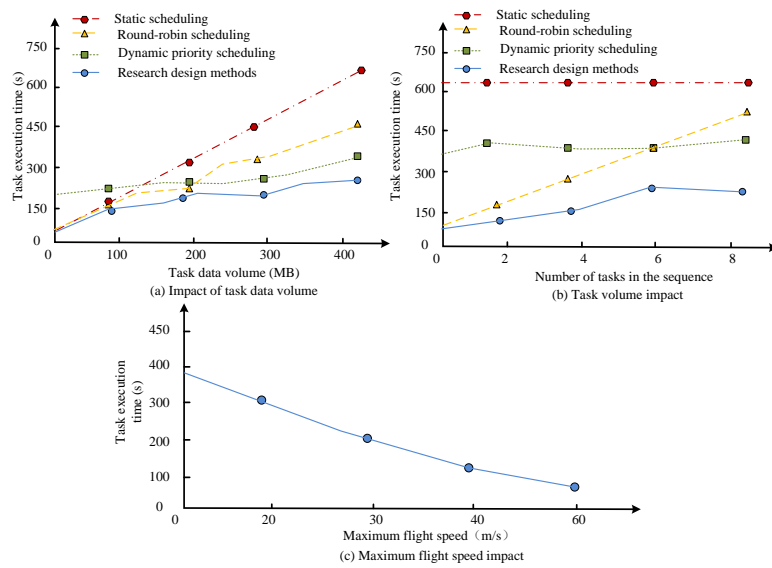


Figure 9: Comparison of task execution time

In Figure 9 (a), the design method always had the shortest execution time under changes in task data volume. From Figure 9 (b), the research design method dynamically adjusted the execution time under changes in

task volume. This method maintained a minimum and ultimately decreased, indicating optimization of task execution sequence. From Figure 9 (c), the faster the flight time, the faster the task completion speed.

Table 5: Comparison of average operation time (s)

Optimization model	Minimum map size	Medium map size	Maximum map size	Average calculation time
NSGA-III	55.0	130.4	500.0	228.4
IDRLO	58.9	140.5	545.3	248.2
ENNO	60.5	125.7	540.2	242.1

From Table 5, the NSGA-III model had the shortest average computation time and was the most superior. The superiority of this computation time was reflected in large, medium, and small maps.

5 Discussion

This study is based on the NSGA-III algorithm and focuses on the task configuration and path planning problems of UAV under limited resource conditions. In the results, the processing efficiency and scheduling effect of multi-objective scheduling problems were significantly improved under limited airborne conditions of UAV. In similar fields, the Thomas T team solved the routing and scheduling problems of single truck multi-UAV delivery systems using mixed integer linear programming and RF-RRO heuristic methods, mainly optimizing delivery time and cost [18]. Sun F et al. applied the dragonfly algorithm for UAV task scheduling in agricultural plant protection environments, focusing on the timeliness of task execution [19]. The Ms index of this study reached 0.881 in large-scale map testing, and the performance of the model in practical applications was better than NSGA-II and SA. Meanwhile, the

designed model had a shorter computation time, demonstrating higher computational efficiency. Meanwhile, the computational efficiency of the research model on large-scale maps is excellent. Therefore, this designed model had advantages in computational efficiency and MOO. This method not only improved the efficiency and quality of UAV scheduling systems, but also provided a new perspective for solving similar problems.

This study provides effective solutions for the application of UAV systems in commercial logistics, disaster response and rescue, environmental monitoring, and agricultural management. Therefore, flight path planning, task allocation, and charging station management can be addressed. This study not only improves the efficiency of drone scheduling, but also significantly improves computational efficiency. Therefore, UVA can minimize resource consumption and flight risks while ensuring task execution under limited onboard conditions. This study can be used for UAV disaster assessment, wounded search, and emergency supplies transportation in natural disaster rescue operations. The research method can be used for environmental monitoring and precision agriculture

monitoring, allowing operators to reduce operating costs and collect data more efficiently. In UVA warfare, this method can improve the efficiency of drone military reconnaissance, surveillance, and strike. Then task execution speed and accuracy efficiency can be improved in complex and resource scarce environments. Meanwhile, the real-time response capability of combat units can be enhanced. In terms of scalability, in the future, injection task allocation, path planning, charging management, and other functions can be modularized. At the same time, more improvements can be made for special environments to enhance the overall flexibility of the system.

6 Conclusion

The study proposed an integrated mathematical model framework for more efficient planning of UAV flight paths, task allocation, and management of charging stations. This framework adopted NSGA-III to implement scheduling strategies based on factors such as task characteristics, UAV resource capabilities, map size, and flight parameters. These results confirmed that the designed model exhibited superiority in multiple key performance indicators. In large maps, NSGA-III achieved a Ms index of 0.881, higher than NSGA-II and SA. On a medium-sized map, its Aq index reached 0.133. In addition, the calculation time of this research model on small maps was 58.9 seconds, which was lower than other models. On a medium-sized map, its calculation time was only 140.5 seconds, compared to an IGA of 158.9 seconds. Specifically, NSGA-III had a computation time of 545.3 seconds on large maps, which had an advantage in computational efficiency. In summary, the research model not only shows significant efficiency in dealing with UAV multi-objective task scheduling problems, but also performs equally well in scheduling quality and time management.

References

- [1] H. Sun, B. Zhang, X. Zhang, Yu. Ying, K. W. Sha, and W. S. Shi, "FlexEdge: Dynamic task scheduling for a UAV-Based on-demand mobile edge server," *IEEE Internet of Things Journal*, vol. 9, no. 17, pp. 15983-16005, 2022. <https://doi.org/10.1109/JIOT.2022.3152447>
- [2] Z. Liu, Y. Cao, P. Gao, X. H. Hua, D. C. Zhang, and T. Jiang, "Multi-UAV network assisted intelligent edge computing: Challenges and opportunities," *China Communications*, vol. 19, no. 3, pp. 258-278, 2022. <https://doi.org/10.23919/JCC.2022.03.019>
- [3] U. A. Bukar, M. S. Sayeed, S. F. A. Razak, S. Yogarayan, and O. A. Amodu, "An exploratory bibliometric analysis of the literature on the age of information-aware unmanned aerial vehicles aided communication," *Informatica*, vol. 47, no. 7, pp. 91-114, 2023. <https://doi.org/10.31449/inf.v47i7.4783>
- [4] C. Zhu, G. Zhang, and K. Yang, "Fairness-aware task loss rate minimization for multi-UAV enabled mobile edge computing," *IEEE Wireless Communications Letters*, vol. 12, no. 1, pp. 94-98, 2022. <https://doi.org/10.1109/LWC.2022.3218035>
- [5] J. Zhang, M. Li, Z. Chen, and B. Lin, "Computation offloading for object-oriented applications in a UAV-based edge-cloud environment," *The Journal of Supercomputing*, vol. 78, no. 8, pp. 10829-10853, 2022. <https://doi.org/10.1007/s11227-021-04288-0>
- [6] J. Chen, X. Qing, F. Ye, K. Xiao, K. You, and Q. Sun, "Consensus-based bundle algorithm with local replanning for heterogeneous multi-UAV system in the time-sensitive and dynamic environment," *The Journal of Supercomputing*, vol. 78, no. 2, pp. 1712-1740, 2022. <https://doi.org/10.1007/s11227-021-03940-z>
- [7] Z. Wei, M. Zhu, N. Zhang, L. Wang, Y. Y. Zou, Z. Y. Meng, H. C. Wu, and Z. Y. Feng, "UAV-assisted data collection for internet of things: A survey," *IEEE Internet of Things Journal*, vol. 9, no. 17, pp. 15460-15483, 2022. <https://doi.org/10.1109/JIOT.2022.3176903>
- [8] W. Liu, K. Quijano, and M. M. Crawford, "YOLOv5-Tassel: Detecting tassels in RGB UAV imagery with improved YOLOv5 based on transfer learning," *IEEE Journal of Selected Topics in Applied Earth Observations and Remote Sensing*, vol. 15, pp. 8085-8094, 2022. <https://doi.org/10.1109/JSTARS.2022.3206399>
- [9] S. Pal, A. Roy, P. Shivakumara, and U. Pal, "Adapting a swin transformer for license plate number and text detection in drone images," *Artificial Intelligence and Applications*, vol. 1, no. 3, pp. 145-154, 2023. <https://doi.org/10.47852/bonviewAIA3202549>
- [10] W. You, C. Dong, Q. Wu, Y. B. Qu, Y. L. Wu, and R. He, "Joint task scheduling, resource allocation, and UAV trajectory under clustering for FANETs," *China Communications*, vol. 19, no. 1, pp. 104-118, 2022. <https://doi.org/10.23919/JCC.2022.01.009>
- [11] S. Halder, A. Ghosal, and M. Conti, "Dynamic super round-based distributed task scheduling for UAV networks," *IEEE Transactions on Wireless Communications*, vol. 22, no. 2, pp. 1014-1028, 2022. <https://doi.org/10.1109/TWC.2022.3200366>
- [12] Z. Niu, H. Liu, X. Lin, and J. Z. Du, "Task scheduling with UAV-assisted dispersed computing for disaster scenario," *IEEE Systems Journal*, vol. 16, no. 4, pp. 6429-6440, 2022. <https://doi.org/10.1109/JSYST.2021.3139993>
- [13] Y. Wang, X. Wei, H. Wang, J. H. Fan, J. Chen, K. Zhao, and Y. Y. Hu, "Joint UAV deployment, SF placement, and collaborative task scheduling in heterogeneous multi-UAV-empowered edge intelligence," *IET Communications*, vol. 17, no. 5, pp. 641-657, 2023. <https://doi.org/10.1049/cmu2.12570>

- [14] I. Khettabi, L. Benyoucef, and M. Amine Boutiche, “Sustainable multi-objective process planning in reconfigurable manufacturing environment: Adapted new dynamic NSGA-II vs new NSGA-III,” *International Journal of Production Research*, vol. 60, no. 20, pp. 6329-6349, 2022. <https://doi.org/10.1080/00207543.2022.2044537>
- [15] M. Awad, M. Abouhawwash, and H. N. Agiza, “On NSGA-II and NSGA-III in portfolio management,” *Intelligent Automation and Soft Computing*, vol. 32, pp. 1893-1904, 2022. <https://doi.org/10.32604/iasc.2022.023510>
- [16] N. N. Johnson, V. Madhavadas, B. Asati, A. Giri, S. A. Hanumant, N. Shajan, and K. S. Arora, “Multi-objective optimization of resistance spot welding parameters of BH340 steel using Kriging and NSGA-III,” *Transactions of the Indian Institute of Metals*, vol. 76, no. 11, pp. 3007-3020, 2023. <https://doi.org/10.1007/s12666-023-03051-8>
- [17] S. Harif, G. Azizyan, M. Dehghani Darmian, and G. Mohammad, “Selecting the best location of water quality sensors in water distribution networks by considering the importance of nodes and contaminations using NSGA-III (case study: Zahedan water distribution network, Iran),” *Environmental Science and Pollution Research*, vol. 30, no. 18, pp. 53229-53252, 2023. <https://doi.org/10.21203/rs.3.rs-1938809/v1>
- [18] T. Thomas, S. Srinivas, and C. Rajendran, “Collaborative truck multi-drone delivery system considering drone scheduling and en route operations,” *Annals of Operations Research*, pp. 1-47, 2023. <https://doi.org/10.1007/s10479-023-05418-y>
- [19] F. Sun, X. Wang, and R. Zhang, “Task scheduling system for UAV operations in agricultural plant protection environment,” *Journal of Ambient Intelligence and Humanized Computing*, pp. 1-15, 2020. <https://doi.org/10.1007/s12652-020-01969-1>